Involvement of the Rho–mDia1 pathway in the regulation of Golgi complex architecture and dynamics

Yuliya Zilberman[a], Naila O. Alieva[b], Stéphanie Miserey-Lenkei[c], Alexandra Lichtenstein[a], Zvi Kam[a], Helena Sabanay[a], and Alexander Bershadsky[a,b]

[a]Department of Molecular Cell Biology, Weizmann Institute of Science, Rehovot, Israel; [b]Mechanobiology Institute, National University of Singapore, Singapore; [c]Institut Curie–Centre National de la Recherche Scientifique UMR 144, Paris, France

ABSTRACT **In mammalian cells, the Golgi apparatus is a ribbon-like, compact structure composed of multiple membrane stacks connected by tubular bridges. Microtubules are known to be important to Golgi integrity, but the role of the actin cytoskeleton in the maintenance of Golgi architecture remains unclear. Here we show that an increase in Rho activity, either by treatment of cells with lysophosphatidic acid or by expression of constitutively active mutants, resulted in pronounced fragmentation of the Golgi complex into ministacks. Golgi dispersion required the involvement of mDia1 formin, a downstream target of Rho and a potent activator of actin polymerization; moreover, constitutively active mDia1, in and of itself, was sufficient for Golgi dispersion. The dispersion process was accompanied by formation of dynamic F-actin patches in the Golgi area. Experiments with cytoskeletal inhibitors (e.g., latrunculin B, blebbistatin, and Taxol) revealed that actin polymerization, myosin-II–driven contractility, and microtubule-based intracellular movement were all involved in the process of Golgi dispersion induced by Rho–mDia1 activation. Live imaging of Golgi recovery revealed that fusion of the small Golgi stacks into larger compartments was repressed in cells with active mDia1. Furthermore, the formation of Rab6-positive transport vesicles derived from the Golgi complex was enhanced upon activation of the Rho–mDia1 pathway. Transient localization of mDia1 to Rab6-positive vesicles was detected in cells expressing active RhoA. Thus, the Rho–mDia1 pathway is involved in regulation of the Golgi structure, affecting remodeling of Golgi membranes.**

Monitoring Editor
Laurent Blanchoin
CEA Grenoble

Received: Jan 5, 2011
Revised: May 25, 2011
Accepted: Jun 7, 2011

INTRODUCTION

Organization of Golgi components into a single complex localized in the perinuclear cell area in the proximity of the centrosome is a characteristic feature of mammalian cells (Thyberg and Moskalewski, 1999; Glick and Nakano, 2009; Sutterlin and Colanzi, 2010). How such an organization is developed and maintained, however, is poorly understood. Several factors are known to be integral to Golgi complex organization. The matrix proteins GRASP65, GRASP55, GM130, and GMAP210 are believed to tether Golgi cisternae to each other and keep them together (Ramirez and Lowe, 2009; Sengupta *et al.*, 2009). In addition, the cytoskeleton plays an important role in the maintenance of Golgi architecture and its proper positioning in the cell.

The role of microtubules has been studied extensively for decades (for review see Thyberg and Moskalewski, 1999; Sutterlin and Colanzi, 2010). Microtubule depolymerization by means of nocodazole and other related drugs leads to rapid deterioration of the Golgi structure and the appearance of newly formed Golgi ministacks at endoplasmic reticulum (ER) exit sites scattered throughout the cell (Cole *et al.*, 1996; Storrie *et al.*, 1998; Thyberg and Moskalewski, 1999). Recovery of the Golgi following drug removal depends on the directional, retrograde movement of these ministacks along microtubules, their

This article was published online ahead of print in MBoC in Press (http://www.molbiolcell.org/cgi/doi/10.1091/mbc.E11-01-0007) on June 16, 2011.

Address correspondence to: Alexander Bershadsky (alexander.bershadsky@weizmann.ac.il).

Abbreviations used: ADF, actin depolymerizing factor; ER, endoplasmic reticulum; GalT-YFP, N-terminal fragment of β-galactosiltransferase fused to yellow fluorescent protein (a marker for *trans*-Golgi); GFP, green fluorescent protein; Lifeact, a 17-amino-acid peptide, which stained filamentous actin (F-actin); LIMK, LIM domain kinase; LPA, lysophosphatidic acid; ManII-GFP, a Golgi enzyme mannosidase II fused to green fluorescent protein (a *cis*/medial-Golgi marker); mCherry-Lifeact, mCherry fluorescent protein fused to Lifeact, a probe for F-actin; mDia1ΔN3, a truncated constitutively active derivative of mDia1; ROCK, Rho-associated protein kinase; VSVG, vesicular stomatitis virus glycoprotein.

accumulation in the pericentrosomal area, and their subsequent fusion into ribbons (Thyberg and Moskalewski, 1999; Miller *et al.*, 2009). Both radial microtubule arrays nucleated by the centrosome and microtubules nucleated or stabilized by the Golgi elements themselves (Chabin-Brion *et al.*, 2001; Efimov *et al.*, 2007; Hoppeler-Lebel *et al.*, 2007; Rivero *et al.*, 2009) participate in the recovery of the Golgi ribbon structure (Hoppeler-Lebel *et al.*, 2007; Miller *et al.*, 2009). In some cell types treated with the microtubule-stabilizing drug Taxol (Schiff and Horwitz, 1980), remodeling of the Golgi ribbons also occurs (Wehland *et al.*, 1983; Hoshino *et al.*, 1997); however, this process is slower and leads to a lower degree of fragmentation than Golgi dispersion induced by microtubule depolymerization.

Movement of Golgi elements along microtubules depends on microtubule-based molecular motors. Among these are cytoplasmic dynein (Corthesy-Theulaz *et al.*, 1992; Burkhardt, 1998; Thyberg and Moskalewski, 1999; Allan *et al.*, 2002) and several kinesins (Echard *et al.*, 1998; Xu *et al.*, 2002; Stauber *et al.*, 2006; Gupta *et al.*, 2008). The dynactin molecular complex, linking the microtubule motors with various cargos, including Golgi membrane elements (Schroer, 2004), was shown to be required for the maintenance of the Golgi architecture (Burkhardt *et al.*, 1997; Burkhardt, 1998).

In addition to microtubules, the actin cytoskeleton seems to affect Golgi architecture and positioning. Structural information concerning the association of actin filaments with Golgi membranes is limited, although immuno–electron microscopy revealed β- and γ-actin at the Golgi-associated COPI-coated buds (Valderrama *et al.*, 2000), and short filaments decorated with the tropomyosin isoform Tm5NM-2 were detected at the budding zones on the ends of Golgi cisternae (Percival *et al.*, 2004). Other studies suggest that the Golgi membrane might be surrounded by a spectrin–actin network, similar to that underlying the erythrocyte membrane (Beck and Nelson, 1998; Holleran and Holzbaur, 1998; De Matteis and Morrow, 2000; Kang *et al.*, 2009).

A number of agents that affect the polymerization status of actin filaments were shown to perturb Golgi morphology and integrity. In particular, in several types of cultured cells, actin depolymerization by means of C2 botulinum toxin, cytochalasin D, or latrunculin B led to compaction of the Golgi and an apparent reduction in its projected area (Valderrama *et al.*, 1998; Lazaro-Dieguez *et al.*, 2006). Electron microscopy studies revealed the swelling of Golgi cisternae in such cells (Lazaro-Dieguez *et al.*, 2006). This effect seems to be cell-type specific, since in cells of neural origin, latrunculin and cytochalasin produced dispersion of the Golgi complex rather than its compaction (Camera *et al.*, 2003; Rosso *et al.*, 2004).

Both myosin-driven actin movement and actin polymerization can affect Golgi organization and dynamics. Myosin VI localizes to the Golgi and is essential to normal Golgi morphology (Warner *et al.*, 2003; Sahlender *et al.*, 2005). Myosin 18 interacts with the Golgi membrane phospholipid phosphatidylinositol-4-phosphate via the GOLPH3 linker and controls the flattened shape of Golgi cisternae (Dippold *et al.*, 2009). Myosin II is associated with Golgi membranes via interaction with Rab6, a Golgi-specific G-protein, and is involved in Golgi membrane fission (Miserey-Lenkei *et al.*, 2010). Myosin 1b was recently shown to promote the formation of post-Golgi carriers (Almeida *et al.*, 2011).

Experimental manipulations with several proteins that regulate the dynamics of actin filaments also produced structural and functional alterations in the Golgi apparatus. Both activation and knockdown of the actin-depolymerizing factor ADF/cofilin produce specific changes in Golgi-mediated secretion and trafficking events (Salvarezza *et al.*, 2009; von Blume *et al.*, 2009). A major regulator of cofilin, LIM kinase 1, was shown to be localized at the Golgi (Foletta *et al.*, 2004) and affect its dynamics via cofilin phosphorylation (Rosso *et al.*, 2004; Salvarezza *et al.*, 2009). Actin filament nucleation by means of the Arp2/3 complex may also control Golgi organization and function. Indeed, the WHAMM protein (WASP homologue associated with actin, membranes, and microtubules), a novel actin nucleation-promoting factor that activates the Arp2/3 complex, was shown to associate with Golgi membranes and regulate Golgi architecture and ER-to-Golgi transport (Campellone *et al.*, 2008).

Formin-family proteins stimulate both nucleation and elongation of actin filaments (Chhabra and Higgs, 2007; Goode and Eck, 2007; Chesarone *et al.*, 2010). In particular, mammalian Diaphanous-related formin 1 (mDia1), a direct target of small GTPase Rho (Watanabe *et al.*, 1997), is a potent activator of actin polymerization in vitro (Li and Higgs, 2003). The Diaphanous-related formins, and specifically mDia1, were shown to be involved in a variety of in vivo functions (for review see Narumiya *et al.*, 2009; Chesarone *et al.*, 2010), which include regulation of both cell polarity and intracellular trafficking of vesicles and organelles (Magdalena *et al.*, 2003; Fernandez-Borja *et al.*, 2005; Minin *et al.*, 2006; Yamana *et al.*, 2006; Wallar *et al.*, 2007; Shi *et al.*, 2009).

In the present study, we address the effects of mDia1 and its activator, RhoA, on the architecture and dynamics of the Golgi apparatus. We found that activation of the Rho–mDia1 pathway indeed induced marked reorganization of the Golgi, which depends on the actin cytoskeleton and can be greatly enhanced by the microtubule-stabilizing drug Taxol. We present evidence that Rho–mDia1 is involved in regulating the fusion of the Golgi membranes and formation of Rab6-positive Golgi-derived transport carriers and plays a critical role in Golgi complex integrity.

RESULTS

Activation of RhoA induces dispersion of the Golgi complex

In HeLa JW cells (Paran *et al.*, 2006), expression of a constitutively active mutant of RhoA (RhoA-V14) produces a marked alteration in Golgi complex organization.

Labeling of Golgi with the *trans*-Golgi marker GalT–yellow fluorescent protein (YFP) (YFP fused to the N-terminus of β-galactosyltransferase) revealed disruption of the Golgi ribbon structure into smaller elements dispersed from the narrow perinuclear area over the entire central part of the cell (Figure 1A, top). A similar effect was observed using markers of medial Golgi (mannosidase II–green fluorescent protein [GFP]) or *cis*-Golgi (endogenous p115, Grasp65) (see Figures 3 and 6 later and Supplemental Figures S1–S3). The active form of RhoB also triggered Golgi dispersion, whereas another small GTPase, Rac, did not produce any effect on Golgi morphology (unpublished data).

Lysophosphatidic acid (LPA) treatment is known to rapidly activate Rho (Ren *et al.*, 1999); its activation made it possible to track the dynamics of Golgi reorganization. Experiments with LPA stimulation were performed in serum-free medium (Ren *et al.*, 1999); serum starvation by itself did not decrease the Golgi compactness (Figure 1, C and D). Time-lapse filming of control cells showed that Golgi elements were mobile, but overall ribbon organization remained generally unchanged throughout the observation period (Supplemental Movie S1). Time-lapse filming of LPA-treated cells revealed the dispersion and centrifugal movement of the Golgi elements. In less than 2 h, the ribbons underwent fragmentation into smaller elements that dispersed radially outward from the cell center (Supplemental Movie S2 and Figure 1B, top).

The extent of fragmentation and dispersion of the Golgi was similar to that produced by expression of constitutively active Rho (Figure 1A, top). The degree of Golgi dispersion was quantified

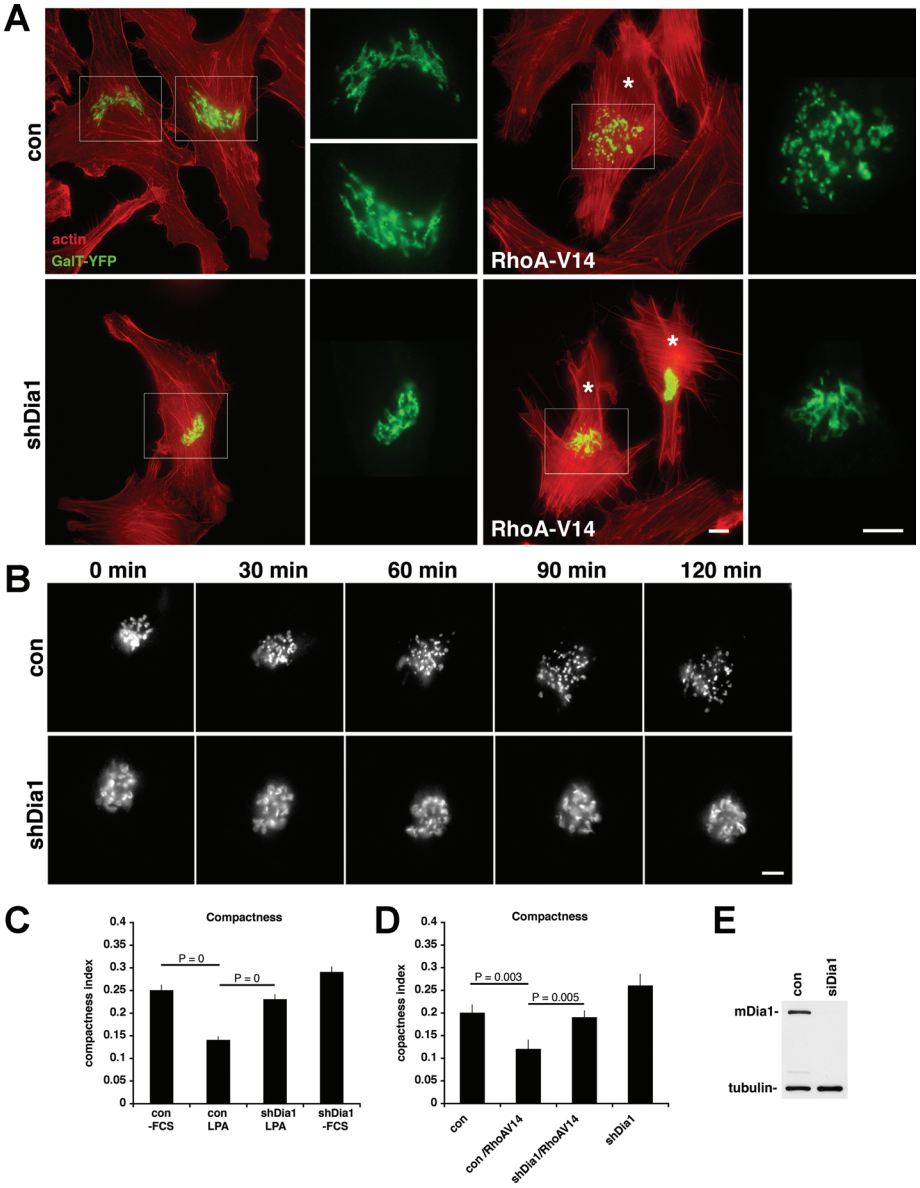

FIGURE 1: Golgi dispersion induced by active RhoA is an mDia1-dependent process. (A, B) Control HeLa JW cells (con) and mDia1 knockdown cells (shDia1) were either (A) transfected with constitutively active Rho (RhoA-V14) and fixed 24 h later or (B) treated with RhoA activator LPA (12 μM) in serum-free medium and filmed for 2 h (see Supplemental Movie S2). (A) Golgi was visualized by transfection with *trans*-Golgi marker GalT-YFP (green; see also the enlarged insets) and actin by staining with phalloidin (red). RhoA-V14–transfected cells in A are marked by white asterisks. In B Golgi was visualized by ManII-GFP. Scale bars, (A) 10 μm, (B) 10 μm. (C, D) Degree of Golgi dispersion was quantified using a compactness (circularity) index calculated on the basis of morphometric measurements (Bard *et al.*, 2003; see also *Materials and Methods*). Bars represent compactness values ± SEM. The p values were calculated according to Student's *t test*. (C) Compactness values for control (con) and mDia1-knockdown (shDia1) cells treated, or not treated, with LPA were measured on fixed specimens stained with p115 *cis*-Golgi marker. (D) Effect of RhoA-V14 on Golgi compactness in control (con) and Dia1-knockdown (shDia1) cells. (E) Western blot illustrating the depletion of mDia1 in HeLa JW cells expressing mDia1-targeted shRNA.

using the index of "compactness" or "circularity" (Bard *et al.*, 2003); the value of this index dropped twofold both in cells treated with LPA and in cells expressing constitutively active Rho (Figure 1, C and D).

Effects of active RhoA on Golgi organization requires mDia1

Because mDia1 is a well-known primary target of Rho, we investigated whether Rho-induced Golgi dispersion is mediated by this Rho effector. To this end, we examined whether constitutively active RhoA or LPA treatment would affect Golgi organization in mDia1 knockdown cells (Figure 1). A HeLa JW cell line stably expressing a vector encoding shRNA for mDia1 (Carramusa *et al.*, 2007) was used in these experiments. The level of mDia1 expression in these cells decreased more than 90%, as revealed by Western blotting (Figure 1E). We found that neither transfection with active RhoA nor treatment with LPA led to significant dispersion of the Golgi in mDia1-depleted cells (Figure 1, A and B, bottom). Our measurements revealed that Golgi compactness in mDia1 knockdown cells treated with LPA or transfected with constitutively active Rho did not differ from that in control cells (Figure 1, C and D). Of note, in mDia1 knockdown cells with nonstimulated RhoA, a slight increase in compactness above control levels was detected. In line with these results, we found that RhoA activation led to the enrichment of mDia1-GFP in the cell area occupied by the Golgi complex (Supplemental Figure S1).

Active mDia1 induces Golgi dispersion in an actin polymerization– and myosin II–dependent manner

Golgi dispersion in LPA-treated cells is accompanied by the transient appearance of F-actin patches in the proximity of Golgi elements, as revealed by live imaging of mCherry-LifeAct–labeled cells (Supplemental Movie S3). To determine whether the effect of active mDia1 on Golgi integrity depends on actin polymerization, we treated cells with the actin polymerization inhibitor latrunculin B (Morton *et al.*, 2000) and observed that such treatment reverses the effect of mDia1 on Golgi dispersion (Figure 2).

Transfection of cells with a constitutively active truncated construct of mDia1 known as mDia1ΔN3 (Watanabe *et al.*, 1999) produced the apparent dispersion of Golgi to an even more pronounced degree than that induced by Rho activation (Figure 2A, left; also see Figure 6A later). Latrunculin increased Golgi compactness, in agreement with previous results (Lazaro-Dieguez *et al.*, 2006) (Figure 2A, top right panel, and Figure 2B), whereas mDia1ΔN3 significantly decreased this morphometric parameter (Figure 2B). In cells expressing mDia1ΔN3, a gradual increase in LatB concentration reduced the mDia1 effect, returning Golgi compactness to control levels at 10 μM (Figure 2B). Taken together, these findings show that Rho-induced Golgi fragmentation is mediated by activation of mDia1; moreover, this effect depends on actin polymerization.

Similar to mDia1, myosin II activity is controlled by Rho (Vicente-Manzanares *et al.*, 2009). Cell treatment with blebbistatin, an

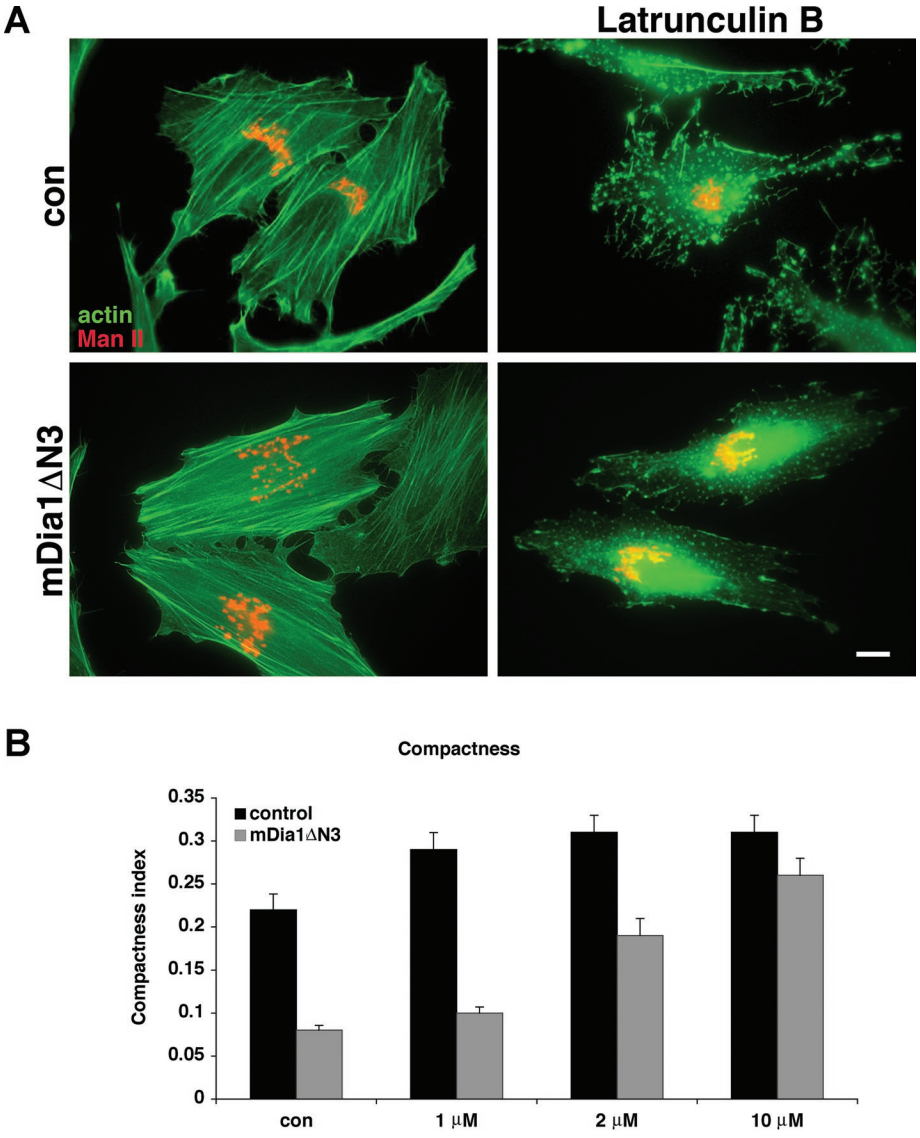

FIGURE 2: An active form of mDia1 (mDia1ΔN3) induces Golgi dispersion in an actin polymerization–dependent manner. (A) Cells were transfected with Golgi marker ManII-GFP, shown in red (con), or cotransfected with ManII-GFP and constitutively active mDia1 (mDia1ΔN3). Latrunculin B at 2 μM concentration was added 24 h after transfection; cells were fixed 2 h later. F-Actin was visualized by phalloidin staining (green). Scale bar, 10 μm. (B) Dispersion of Golgi induced by mDia1ΔN3 is gradually reduced in cells treated with ascending concentrations of latrunculin B. Complete return of the compactness value to control levels was observed in 10 μM latrunculin B–treated, mDia1ΔN3-transfected cells. Error bars in B represent SEM values.

inhibitor of myosin II activity, produced some fragmentation of the Golgi complex (Supplemental Figure S2A). Measurements of Golgi compactness revealed, however, that fragmentation induced by constitutively active mDia1 was significantly more pronounced (Supplemental Figure S2B). Moreover, blebbistatin prevented the decrease of Golgi compactness induced by active mDia1 expression (Supplemental Figure S2, A and B). Thus, mDia1 functions in concert with myosin II in the process of Rho-dependent Golgi fragmentation and dispersion.

Rho and mDia1 activation interfere with the fusion of Golgi elements recovering from nocodazole treatment

Depolymerization of microtubules by nocodazole treatment led to the pronounced disruption of the Golgi complex and the appearance of numerous dispersed Golgi elements (Thyberg and Moskalewski, 1985, 1999). This process requires de novo formation of numerous Golgi ministacks at the cell periphery, presumably at ER exit sites (Cole *et al.*, 1996; Storrie *et al.*, 1998) (Supplemental Movie S4). We found that microtubule depolymerization leads to pronounced Golgi dispersion not only in control cells, but also in mDia1-depleted cells and in cells with active mDia1. This finding enabled us to study how manipulations with Rho and mDia1 affect the recovery of dispersed Golgi following nocodazole removal.

Live imaging of Golgi recovery revealed that this is a two-stage process (Figure 3A and Supplemental Movies S5 and S6). The first stage comprises the rapid centripetal movement of Golgi fragments, leading to their concentration in the perinuclear area. In the second stage, the small fragments coalesce, or "fuse," forming large, ribbon-like structures. We characterized the extent of Golgi complex recovery by measuring the average size (projected area) of individual Golgi fragments and the average number of such fragments per cell (Figure 3B).

The rate of fusion between Golgi elements during the second stage of recovery differed, depending on mDia1 and RhoA status. The fusion rate was maximal in mDia1 knockdown cells and eventually led to the efficient and rapid recovery of the Golgi in such cells (Figure 3A and Supplemental Movie S5). Control cells displayed a somewhat slower fusion rate (Figure 3A and Supplemental Movie S5), whereas the fusion of Golgi elements in cells expressing active Rho or active mDia1 was inefficient (Figure 3A, Supplemental Figure S3, and Supplemental Movie S6). These conclusions were supported by a rapid decrease in number and increase in size of Golgi elements in both mDia1-knockdown cells and in control cells (Figure 3B). At the same time, the number and size of Golgi fragments changed much more slowly in cells expressing active RhoA or active mDia1 (Figure 3, B and C), even though these particles were concentrated in the central part of the cell (Figure 3A, Supplemental Figure S3, and Supplemental Movie S6). These results suggest the involvement of Rho–mDia1 signaling during the fusion of Golgi elements into ribbon-like structures. Cells treated with latrunculin demonstrated slightly more efficient fusion of Golgi elements, in a manner similar to mDia1 knockdown (Figure 3C and Supplemental Figure S3).

Effects of Taxol on Rho-mDia1–mediated Golgi dispersion

We next studied the effect of the microtubule-stabilizing drug Taxol (Schiff and Horwitz, 1980) on Golgi reorganization induced by activation of the RhoA–mDia1 pathway. Surprisingly, Taxol treatment strongly enhanced the Golgi dispersion induced by either

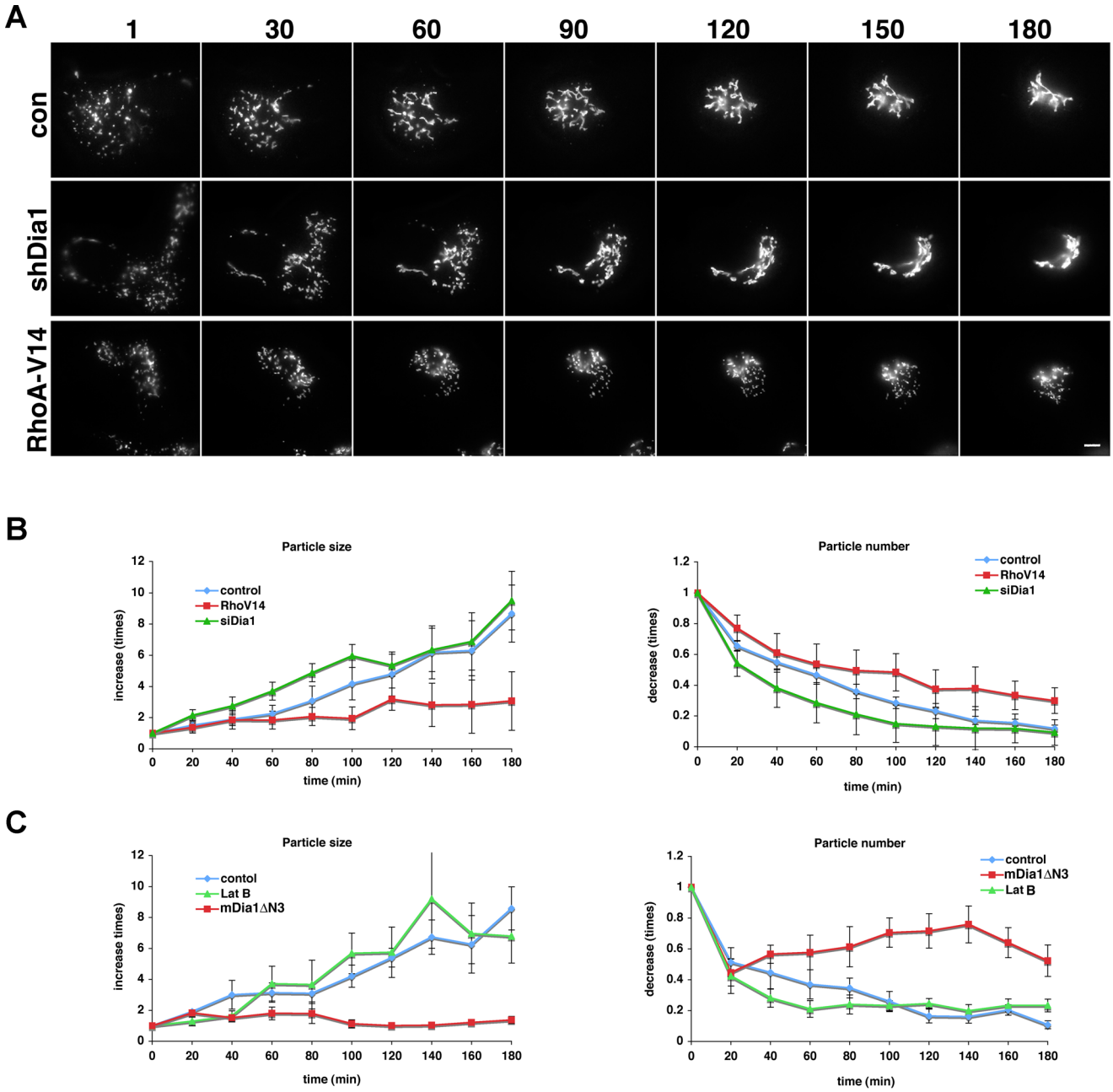

FIGURE 3: Active Rho prevents fusion of Golgi elements into ribbon structures. (A) Cells expressing the Golgi marker ManII-GFP, alone or in combination with plasmids encoding shRNA against mDia1 or constitutively active Rho, were treated with nocodazole (2.5 μM) for 3 h until the Golgi elements were completely dispersed. Nocodazole was then washed out, and the process of Golgi recovery was filmed in a time-lapse manner. Frames from the three time-lapse movies taken for cells of each type at indicated time points are shown in montage A (see Supplemental Movies S5 and S6). Scale bar, 10 μm; time, minutes. Note that even though Golgi elements move centripetally in all cases, efficient fusion of dispersed elements into ribbon structures occurs in control and mDia1 knockdown cells but not in cells expressing active RhoA. (B) Quantification of average size and number of Golgi elements at different time points after nocodazole removal. (C) Quantification of the effect of latrunculin and constitutively active mDia1 (mDia1ΔN3) on the dynamics of Golgi recovery after nocodazole treatment. The corresponding movie frames are shown in Supplemental Figure S3. The data are normalized to their initial value at the zero time point. Particle size (in μm^2) at the zero time point (average ± SD): control (1.3 ± 0.32), RhoV14 (1.3 ± 0.4), siDia1 (1.7 ± 0.4), mDia1ΔN3 (0.54 ± 0.14), and LatB (0.54 ± 0.15). Particle number at the zero time point (average ± SD): control (86 ± 15.8), RhoV14 (66 ± 12.27), siDia1 (64.4 ± 35.9), mDia1ΔN3 (106 ± 61.5), and LatB (57.6 ± 25). For each cell type, 7–10 time-lapse movies were taken for this analysis. Error bars show SD.

mDia1ΔN3 or RhoA-V14 (Figures 4 and 5, Supplemental Movie S7, and unpublished data). Incubation of cells with Taxol for 3 h led to formation of prominent microtubule bundles (Figures 4 and 5), in agreement with previous studies (Schiff and Horwitz, 1980). Live imaging of cells with labeled *trans*-Golgi and microtubules revealed the kinetics of microtubule-dependent Golgi dispersion

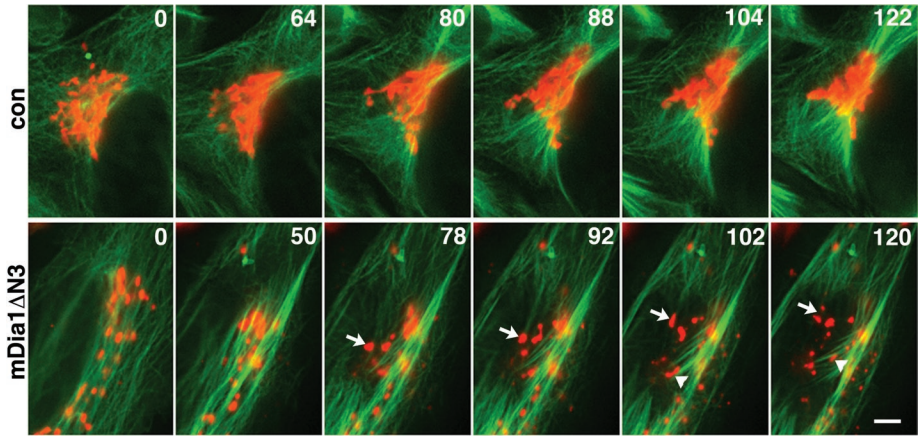

FIGURE 4: Dynamics of Golgi fragmentation and dispersion induced by Taxol in active mDia1-expressing cells. Sequences from time-lapse movies illustrating the effect of Taxol (24 μM) on microtubules (green) and Golgi (red) in a control cell (top) and an mDia1ΔN3-expressing cell (bottom). Microtubules and Golgi were visualized by transfection of cherry-α-tubulin and ManII-GFP, respectively. Time after addition of Taxol is shown in minutes. Note that Taxol treatment leads to the formation of prominent microtubule bundles in both control and mDia1-expressing cells. In control cells, Golgi membranes remain associated with the ends of these bundles and do not undergo fragmentation. In mDia1ΔN3-transfected cells, a large Golgi fragment can move either together with moving bundles (arrows) or along such bundles (arrowheads). The process of fragmentation continues during the course of such movement (see Supplemental Movie S7). Scale bar, 5 μm.

(Figure 4 and Supplemental Movie S7). In Taxol-treated cells that did not contain active mDia1, Golgi elements were concentrated near the ends of the microtubule bundles, usually in the cell center, and displayed essentially normal compact morphology (Figure 4 and Supplemental Movie S7). In Taxol-treated cells expressing the active form of mDia1, newly formed microtubule bundles often moved from the center of the cell to the periphery (Figure 4 and Supplemental Movie S7) along with the Golgi fragments associated with them. This process was accompanied by further fragmentation of Golgi elements (Figure 4 and Supplemental Movie S7). In some cases, Golgi elements moved along microtubule bundles (Figure 4 and Supplemental Movie S7). As a result, cells expressing active mDia1 that were incubated with Taxol for 3 h displayed strong fragmentation of the Golgi complex and dispersion of Golgi elements throughout the entire cell area (Figures 4 and 5).

Enhanced Golgi dispersion induced by Taxol in cells expressing active mDia1 can be prevented by simultaneous treatment of cells with latrunculin B or with the myosin II inhibitor blebbistatin (Figure 5). Thus, Taxol treatment significantly enhanced Golgi fragmentation and dispersion induced by active mDia1, whereas inhibition of actin polymerization or myosin II–driven contractility suppressed both Golgi fragmentation and dispersion.

Golgi fragmentation induced by active Rho and mDia1 leads to formation of Golgi ministacks

To characterize the elements into which the Golgi complex is dispersed under conditions of Rho or mDia1 activation, we visualized the *cis*- and *trans*-Golgi compartments using corresponding markers (the *trans*-Golgi marker GalT-YFP and the *cis*-Golgi marker p115). As described in previous studies, *cis*- and *trans*-Golgi compartments are spatially separated but adjacent to each other (Rothman, 1981; Glick and Nakano, 2009). Analysis of Golgi organization upon activation of Rho or mDia1 under various experimental conditions (Figure 6) revealed that even the smallest fragments of Golgi contained both *cis* and *trans* compartments. In particular, the fragments resulting from maximal Rho-mDia1–mediated Golgi fragmentation (in cells expressing active RhoA and treated with Taxol) still consisted of spatially separated regions positive for *cis* and *trans* markers (Figure 6A). The immunofluorescence observations were confirmed by transmission electron microscopy of control cells and cells expressing active mDia1. In both cases, Golgi stack structures were seen in the cells, even though in cells expressing mDia1ΔN3 they were smaller and slightly swollen (Figure 6B). Thus, Golgi dispersion induced by Rho–mDia1 activation led to the production of ministacks rather than the separation of the Golgi complex into individual cisternae.

The Rho–mDia1 pathway is involved in the formation of Rab6-positive, Golgi-derived vesicles

The small GTPases Rab6A and Rab6A′ localize to the *trans*-Golgi network and mark Golgi-derived exocytotic carriers, as well as vesicles involved in Golgi-to-ER retrograde transport (Martinez *et al.*, 1997; Girod *et al.*, 1999; White *et al.*, 1999; Del Nery *et al.*, 2006; Grigoriev *et al.*, 2007). To gain deeper insights into the functional role of the RhoA–mDia1 pathway in Golgi dynamics, we examined the effects of RhoA activation and mDia1 knockdown on the generation of Rab6A-positive transport carriers (Figure 7 and Supplemental Movies S8 and S9). We found that Rho activation significantly increased the abundance of such vesicles in comparison to control cells (Figure 7, A and B, and Supplemental Movie 8), whereas mDia1 knockdown completely abolished this increase (Figure 7, A and B, and Supplemental Movie S9). Of note, the Rab6A-positive tubular extensions radiating from the Golgi, as well as elongated tubular cytoplasmic vesicles, were more prominent in mDia1 knockdown cells, suggesting a fission defect (Supplemental Movie S9). Active RhoA did not appear to decrease the fraction of these Rab6A-positive tubular elements in mDia1-depleted cells (Supplemental Movie S9).

To determine the mode of action of mDia1 in formation of Rab6-positive vesicles, we used spinning disk confocal microscopy to study the colocalization of GFP-mDia1 and Cherry-Rab6A′ in cells expressing active Rho (RhoA V14). We found that both vesicular and tubular Rab6A′-positive structures often colocalize with small mDia1-positive patches (Figure 8). This colocalization event was very transient (no more than 30 s); however, such events could be seen in almost every frame (Figure 8). We found no colocalization of mDia1 and Rab6A′ in cells that did not express RhoA-V14 (unpublished data). Taken together, these results suggest that RhoA promotes the formation of Rab6-positive vesicles via activation of mDia1, which then transiently colocalizes with these structures.

Because Rab6-positive carriers are involved in exocytosis (Grigoriev *et al.*, 2007), we checked whether mDia1 depletion or activation would affect the exocytosis of a membrane glycoprotein, temperature-sensitive vesicular stomatitis virus glycoprotein (VSVG). We did not detect, however, any differences in VSVG membrane delivery among control cells, cells expressing mDia1ΔN3, and mDia1-knockdown cells (Supplemental Figure S4).

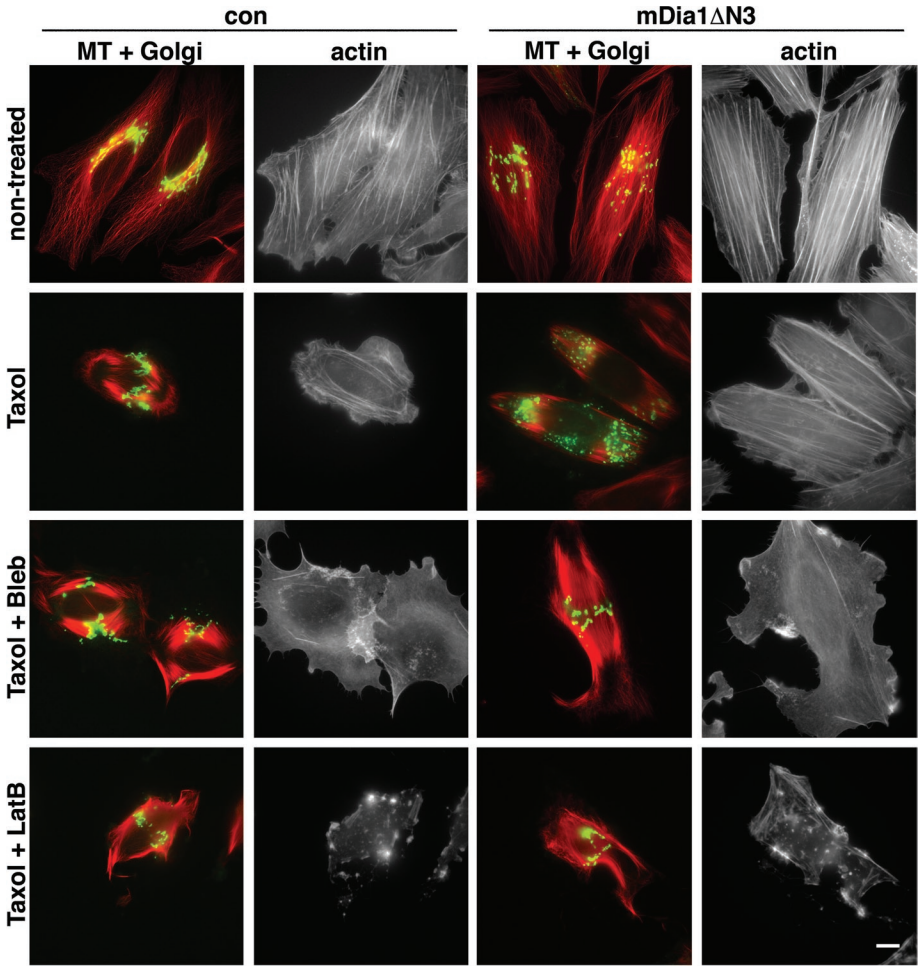

FIGURE 5: Golgi dispersion induced by active mDia1 is enhanced by Taxol in an actin- and myosin II–dependent manner. HeLa JW cells transfected with GalT-YFP Golgi marker (green) alone (con) or together with active mDia1 (mDia1ΔN3) were either left untreated or incubated for 3 h with the microtubule-stabilizing drug Taxol (24 μM) alone (Taxol), with Taxol in combination with blebbistatin (50 μM) (Taxol + Bleb), or with Taxol and latrunculin B (2 μM) (Taxol + LatB). Microtubules (red) and F-actin (black and white photos) were visualized in the same cells by staining with antibody against tubulin and with phalloidin, respectively. Note that Taxol treatment does not induce significant Golgi dispersion in and of itself but strongly stimulates it in cells expressing active mDia1. Both inhibition of actin polymerization by latrunculin B and inhibition of myosin II activity by blebbistatin abolished this effect. Scale bar, 10 μm.

DISCUSSION

The major finding of this study is the discovery of the role of the Rho–mDia1 pathway in the modulation of Golgi architecture. This was demonstrated by experiments showing that constitutively active RhoA, as well as activation of Rho by LPA, appears to fragment the Golgi into ministacks; moreover, such fragmentation can be abolished by mDia1 knockdown. Expression of the active form of mDia1 also leads to similar Golgi fragmentation. The Rho–mDia1 pathway was also shown to be involved in the production of Rab6-positive, Golgi-derived transport vesicles.

What are the mechanisms underlying the regulation of Golgi architecture through the Rho–mDia1 pathway? In search of mDia1 involvement in the local regulation of Golgi membrane sculpting, we examined the dynamics of mDia1 localization vis-à-vis the Golgi structures. We found that upon Rho activation, an mDia1-enriched "cloud" overlaps the Golgi complex. Transient F-actin patches visualized by means of the mCherry-LifeAct were also detected in this area. More definite colocalization of mDia1 and Golgi elements was found in Rab6-positive vesicular and tubular structures.

Furthermore, we determined that the effects of Rho and mDia1 on Golgi architecture depend on actin polymerization and can be abolished by treatment of cells with latrunculin. The enhanced dispersion of the Golgi in our experiments was also inhibited by blebbistatin, indicating myosin II involvement. The mDia1-dependent actin polymerization may, in principle, modify the hypothetical actin–spectrin coat surrounding the Golgi membrane (Beck and Nelson, 1998; Holleran and Holzbaur, 1998), thus affecting the membrane's shape and mechanical characteristics.

Our experiments with Taxol suggest that Rho-mDia1–induced Golgi fragmentation may also depend on the interactions of Golgi membranes with microtubules. Like other formins, mDia1 could, in principle, interact with microtubules either directly or via microtubule-associated proteins (Bershadsky *et al.*, 2006; Bartolini and Gundersen, 2010). Our observations of Golgi fragmentation dynamics in Taxol-treated cells are consistent with the notion that mDia1 might also modify such interactions. Thus, it appears that the Rho–mDia1 pathway controls the actin- and myosin II–mediated processes underlying the shaping and sculpting of Golgi membranes and may coordinate these processes with microtubule-based intracellular movements of the Golgi elements.

Membrane fusion and fission constitute the most basic processes underlying reorganization of complex membrane structures (Luini *et al.*, 2008; Kozlov *et al.*, 2010). Our data suggest that membrane fusion is the main mDia1-dependent process responsible for remodeling the shape of the Golgi complex. Constitutively active mDia1, as well as activation of Rho, inhibits fusion of Golgi fragments, preventing formation of Golgi ribbons in the process of recovery following nocodazole removal. During this process, knockdown of mDia1 somewhat promotes fusion of Golgi fragments.

In addition to suppressing Golgi membrane fusion, there exists some evidence that the Rho–mDia1 pathway helps to trigger fission events. In particular, the formation of Rab6- positive carriers may depend on membrane fission (Miserey-Lenkei *et al.*, 2010). Constitutively active RhoA was shown to augment the production of such vesicles, the majority of which displayed a spherical morphology. In contrast, mDia1 knockdown enhanced the fraction of tubular, Rab6-positive carriers in our experiments. These results, together with localization of mDia1 to the Rab6-positive membrane structures, are consistent with the possible involvement of mDia1 in Golgi membrane fission; however, the molecular and physical mechanisms underlying mDia1-dependent membrane remodeling remain elusive.

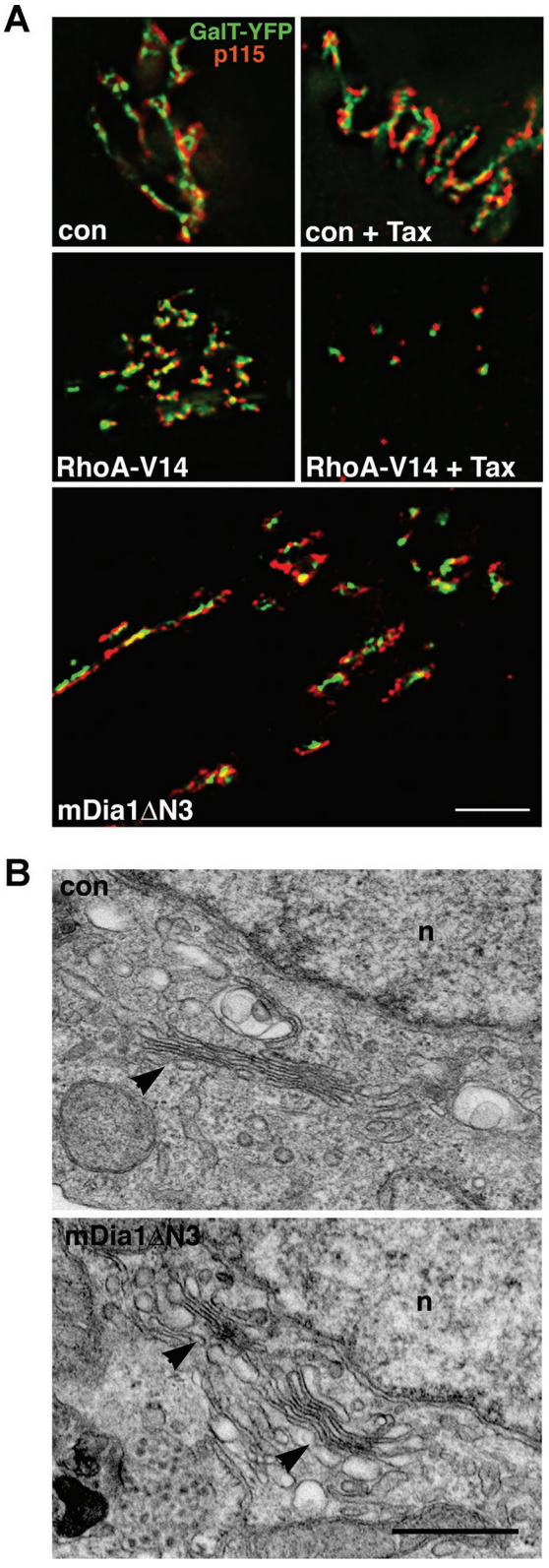

FIGURE 6: Dispersed Golgi elements preserve a ministack structure. (A) The Golgi compartments were labeled by cell transfection with the *trans*-Golgi marker GalT-YFP (green) and immunofluorescence staining with antibody to the *cis*-Golgi marker p115 (red). Nonfragmented Golgi in control or Taxol-treated cells display typical *cis* and *trans* cisternae, forming the ribbon structure. Fragmented Golgi elements in RhoA-V14– or mDia1ΔN3-expressing cells, and even the smallest fragments in RhoA-V14–expressing cells treated with taxol, still preserve joint *cis* and *trans* markers. Scale bar, 10 μm. (B) Transmission electron microscopy of control cells and cells expressing mDia1ΔN3. Arrows indicate the Golgi stacks; n, nucleus. Scale bar, 500 nm. Golgi elements in mDia1ΔN3 cells preserved a stacked structure.

Several recent studies (Salvarezza *et al.*, 2009; von Blume *et al.*, 2009; Miserey-Lenkei *et al.*, 2010) demonstrated the involvement of other Rho-controlled, actin-associated regulatory and effector proteins in the functioning of the Golgi complex. Nonmuscle myosin II is regulated by RhoA via activation of Rho-associated kinase (ROCK) (Vicente-Manzanares *et al.*, 2009). More recently, it was shown that myosin II interacts directly with Rab6 and plays an important role in the formation of Rab6-positive, Golgi-derived transport carriers (Miserey-Lenkei *et al.*, 2010). This finding resembles the effect of the Rho–mDia1 pathway on the formation of the Rab6-positive vesicles found in our study. Our data suggest that RhoA-induced Golgi fragmentation and dispersion depend on both mDia1-driven actin polymerization and myosin II activity.

Another actin-related effector protein apparently involved in Golgi function is the actin depolymerizing protein ADF/cofilin (Rosso *et al.*, 2004; Salvarezza *et al.*, 2009; von Blume *et al.*, 2009). Like mDia1, ADF/cofilin is regulated by a Rho-dependent pathway; thus, active Rho, via ROCK, activates LIM kinases (LIMK1 and LIMK2), which in turn phosphorylate and inactivate cofilin (Bernard, 2007; Bernstein and Bamburg, 2010). The LIMK1–cofilin pathway has been shown to participate in fission regulation (Salvarezza *et al.*, 2009). Finally, another Rho-binding formin, DAAM1, was recently shown to be involved in the regulation of Golgi positioning and perhaps architecture (Ang *et al.*, 2010).

Thus, mDia1 regulates Golgi architecture and dynamics in a Rho-dependent manner, perhaps in concert with other Rho effectors controlling actin polymerization and contractility. Elucidation of the precise molecular and physical mechanisms underlying mDia1 function in these processes is a challenging subject for future study.

MATERIALS AND METHODS

Chemicals and reagents

Nocodazole, latrunculin B, paclitaxel (Taxol), and LPA were purchased from Sigma-Aldrich (St. Louis, MO); blebbistatin from Calbiochem (Merck Eurolab, Darmstadt, Germany); and fibronectin from Biological Industries (Beit-Haemek, Israel).

HeLa JW cells (Paran *et al.*, 2006) and HeLa JW cells stably transfected with cherry α-tubulin (kindly provided by Y. Paran and B. Geiger, Weizmann Institute of Science, Rehovot, Israel) were cultured in DMEM (Rhenium, Jerusalem, Israel) supplemented with 10% fetal calf serum (Biological Industries), L-glutamine, and penicillin–streptomycin solution (Sigma-Aldrich). Trypsin-EDTA (Biological Industries) was used to subculture the cells. Transfections of HeLa JW cells were performed in 36-mm dishes with jetPEI (Polyplus-transfection SA, Illkirch, France) according to the manufacturer's instructions.

Plasmids

The mDia1-Flag, mDia1-GFP, mDia1ΔN3-GFP, and mDia1ΔN3-Flag (Watanabe *et al.*, 1999; Higashida *et al.*, 2004) were kindly provided by S. Narumiya (Kyoto University Faculty of Medicine, Kyoto, Japan). For preparation of monomeric red fluorescent protein (mRFP)–mDia1ΔN3, mRFP was amplified from pRSET-B-RFP plasmid and

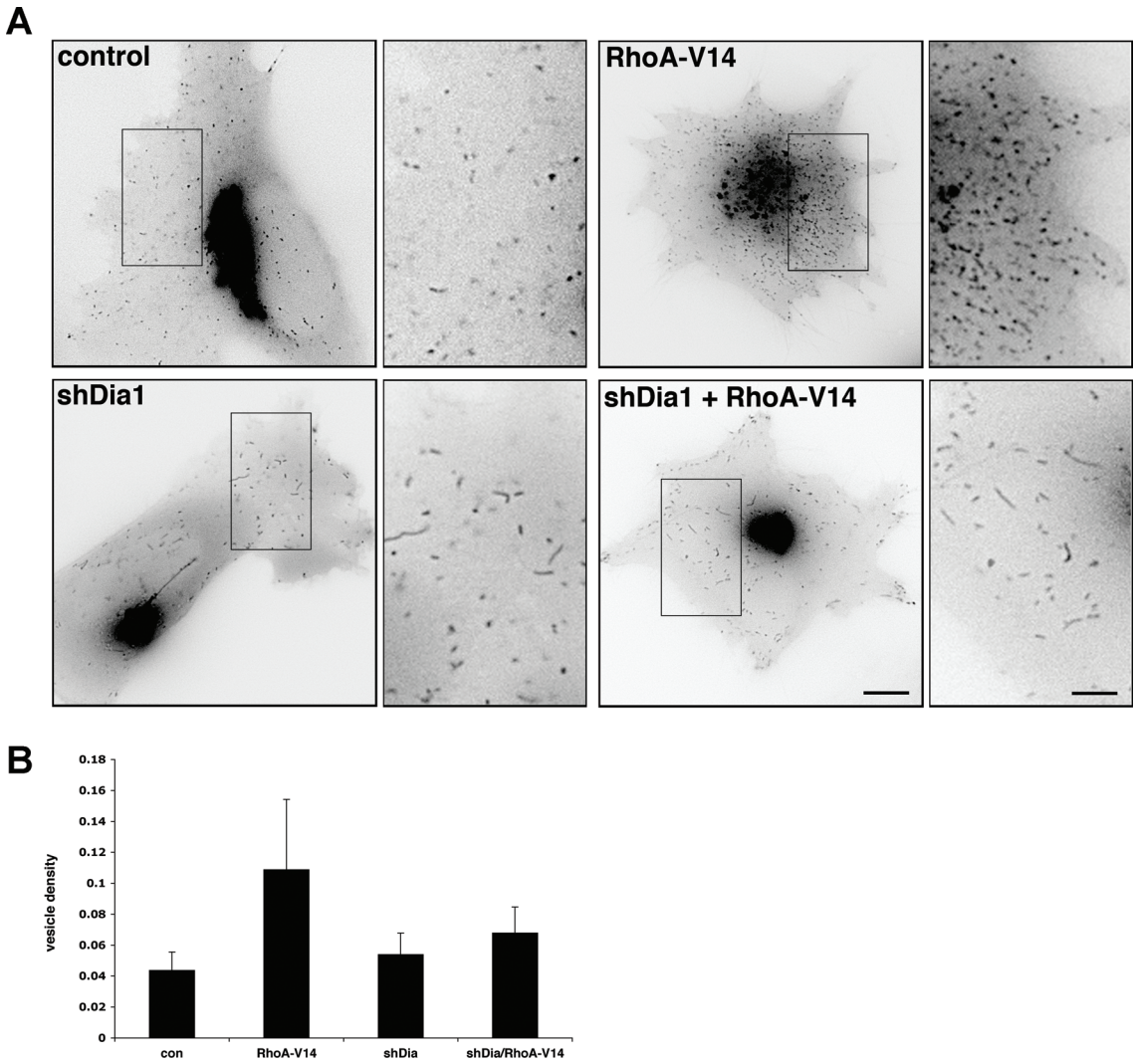

FIGURE 7: Production of Rab6-positive transport carriers is enhanced by active RhoA and inhibited by mDia1 knockdown. (A) Rab6A-GFP was transiently expressed in control HeLa JW cells (con), in cells expressing active RhoA (RhoA-V14), in mDia1 knockdown cells (shDia1), and in mDia1 knockdown cells expressing active RhoA. Rab6A-GFP localizes to Golgi-derived vesicular and tubular carriers. Note the numerous vesicles in control cells expressing RhoA-V14 and the elongated (tubular) morphology of Rab6 membranes in mDia1 knockdown cells with or without active RhoA (insets). Scale bars, 10 and 4 μm (insets). (B) The density of Rab6-positive carriers increases in control but not in mDia1 knockdown cells expressing active RhoA. Error bars show SD.

introduced into mDia1ΔN3-GFP using *Eco*47III/*Xho*I sites instead of GFP. Mannosidase II (ManII)–GFP was a gift from V. Malhotra (Center for Genomic Regulation, Barcelona, Spain). β-GalT-YFP was purchased from Clontech (Mountain View, CA). RhoA-V14 was fused to a VSV tag, as previously described (Helfman *et al.*, 1999). Rab6A-GFP was kindly provided by S. Lev (Weizmann Institute of Science); mCherry-Rab6A′ was kindly provided by F. Perez (Institut Curie, Paris, France); and mCherry-LifeAct (Riedl *et al.*, 2008) was kindly provided by R. Wedlich-Soldner (Max Planck Institute of Biochemistry, Martinsried, Germany).

Knockdown of mDia1

Knockdown of mDia1 was performed using pSuper Dia1-shRNA (shDia1) as well as pSuper-retro-Dia1-shRNA vectors, as described previously (Carramusa *et al.*, 2007). Briefly, a small interfering oligonucleotide specific for human Dia1 and corresponding to its sequence from bases 707-725 (GCATGAGATCATTCGCTGC) was synthesized, annealed and cloned in pSuper plasmids (Brummelkamp *et al.*, 2002). The plasmids produced were then verified by DNA sequencing.

The HeLa JW siDia1 stable cell line was produced by transfection with the pSuper-retro-shDia1 plasmid. Selection was carried out in the presence of 0.4 μg/ml puromycin (Sigma-Aldrich) for 10 d. Western blot analysis of cell lysates showed an ~90% reduction in mDia1 protein in the stably transfected cells. For mDia1 detection, mouse monoclonal antibody (mAb) against p140mDia1 (BD Biosciences, Heidelberg, Germany) was used at a 1:500 dilution in phosphate-buffered saline (PBS). Western blotting of α-tubulin (with the anti–α-tubulin antibody DM1A; Sigma-Aldrich) was used for loading control. Quantification of Western blot signals was performed using ImageJ software (National Institutes of Health, Bethesda, MD).

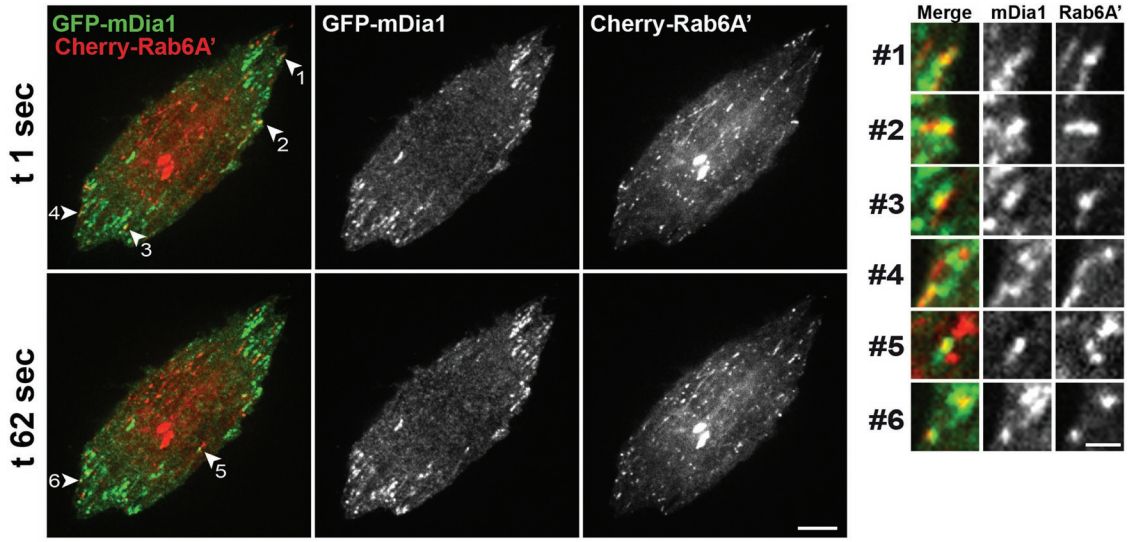

FIGURE 8: Colocalization of mDia1 and Rab6A′ in cells expressing constitutively active RhoA. Cells were triple transfected with GFP-mDia1 (green), Cherry-Rab6A′ (red), and RhoA-V14-VSV (not shown). The colocalization regions in the merged images are colored yellow. The images of the same cell at two different time points are shown in top and bottom rows, respectively. Some sites of colocalization are indicated by arrowheads and numbered. Insets on the right show magnified images corresponding to these colocalization events. Scale bars, 10 and 1.5 μm (insets).

Immunostaining and fluorescence microscopy

After transfection, cells were plated on glass coverslips coated with fibronectin (20 μg/ml). Cells were then cultured for 24 h before treatment with drugs and fixation.

For microtubule visualization, cells were fixed as previously described (Zilberman *et al.*, 2009) and stained using an indirect immunofluorescence method with mouse monoclonal anti–α-tubulin antibody (clone DM1A; Sigma-Aldrich) and Cy3- or Cy5-conjugated goat anti–mouse antibody (Jackson ImmunoResearch Laboratories, West Grove, PA). For mDia1, F-actin, and Golgi visualization, cells were fixed with 3% paraformaldehyde in PBS for 20 min at 37°C and then permeabilized with 0.25% Triton X-100 for 5 min. F-Actin was stained with coumarin–phalloidin (Sigma-Aldrich); mDia1 was stained with the mouse mAb against p140mDia1 (BD Biosciences); and Golgi was stained with mouse anti-p115 or anti-Grasp65 antibodies (a gift from S. Lev).

Fluorescence images were captured with an Olympus IX71 inverted fluorescent microscope equipped with a charge-coupled device camera (CoolSNAP HQ; Photometrics, Tucson, AZ) and controlled by a DeltaVision system (Applied Precision, Issaquah, WA). A dichroic mirror and excitation and emission filter wheels (Chroma Technology, Rockingham, VT) were adjusted for detection of fluorescein isothiocyanate (FITC), 4′,6-diamidino-2-phenylindole, rhodamine, and Cy-5.

Observations of the colocalization of GFP-mDia1 and Cherry-Rab6A′ were carried out using a PerkinElmer spinning-disk confocal microscope based on an inverted Olympus microscope IX81, equipped with a PL FL 100× 1.4–numerical aperture (NA) objective lens, Hamamatsu C9100-13 EMCCD camera for image acquisition, and Volocity software to control the setup (PerkinElmer, Waltham, MA). Acquisition parameters were 100-ms exposure for the 488 channel and 100 ms for the 561 channel. Lasers ware set to 24% in each case. Images were converted into TIFF files by ImageJ software and arranged into figures using Adobe Photoshop (San Jose, CA).

Transmission electron microscopy was performed as described (Levenberg *et al.*, 1998).

Videomicroscopy

Cells transfected with the plasmids listed were replated on fibronectin-coated, glass-bottomed dishes (MatTek Corporation, Ashland, MA) 6 h after transfection and placed on the microscope stage 24-36 h later. Images were recorded on an Olympus IX71 inverted fluorescence microscope equipped with a temperature and CO_2 control unit (Life Imaging Services, Reinach, Switzerland). Objectives used were Olympus plan ApoN 60× 1.42 NA or Olympus 100× 1.3 NA UplanFI. Images were filtered using the Unsharp Mask plug-in of Image J and converted to movies.

Image analysis

Vesicle density was measured using the ImageJ Analyze Particles plug-in applied to the polygon drawn around the cell. Before analysis, images were convolved and thresholded for better vesicle segmentation.

Golgi morphology was quantified using an index of circularity or compactness defined as $4\pi \times \text{Area}/\Sigma\ \text{Perimeter}^2$ (Bard *et al.*, 2003), where Area represents the total Golgi projected area and Σ Perimeter is the sum of the perimeters of all Golgi fragments. All of the parameters were measured per cell. The compactness index approaches the maximal value of 1 for the most compact shape, namely, a circle. At least 30 cells were taken for each measurement.

ACKNOWLEDGMENTS

We are grateful to Benjamin Geiger, Sima Lev, Orly Reiner (Weizmann Institute of Science, Rehovot, Israel), Jim Bamburg (Colorado State University, Fort Collins, CO), and Graham Warren (Max F. Perutz Laboratories, Vienna, Austria) for fruitful discussions and to A. Alberts (Van Andel Research Institute, Grand Rapids, MI), B. Geiger and S. Lev, V. Malhotra (Center for Genomic Regulation, Barcelona, Spain), F. Perez (Institut Curie, Paris, France), R. Wedlich-Soldner (Max Planck Institute of Biochemistry, Martinsried, Germany), and S. Narumiya (Kyoto University, Kyoto, Japan) for providing reagents and materials. The electron microscopy studies were conducted at

the Irving and Cherna Moskowitz Center for Nano and Bio-Nano Imaging (Weizmann Institute of Science). A.D.B. holds the Joseph Moss Professorial Chair in Biomedical Research. His work was partially supported by the Israel Science Foundation, the Minerva Foundation, and the De Benedetti Foundation-Cherasco. The authors are grateful to Barbara Morgenstern for excellent editorial assistance.

REFERENCES

Allan VJ, Thompson HM, McNiven MA (2002). Motoring around the Golgi. Nat Cell Biol 4, E236–E242.

Almeida CG, Yamada A, Tenza D, Louvard D, Raposo G, Coudrier E (2011). Myosin 1b promotes the formation of post-Golgi carriers by regulating actin assembly and membrane remodelling at the trans-Golgi network. Nat Cell Biol 13, 779–789.

Ang SF, Zhao ZS, Lim L, Manser E (2010). DAAM1 is a formin required for centrosome re-orientation during cell migration. PLoS One 5, e13064.

Bard F, Mazelin L, Pechoux-Longin C, Malhotra V, Jurdic P (2003). Src regulates Golgi structure and KDEL receptor-dependent retrograde transport to the endoplasmic reticulum. J Biol Chem 278, 46601–46606.

Bartolini F, Gundersen GG (2010). Formins and microtubules. Biochim Biophys Acta 1803, 164–173.

Beck KA, Nelson WJ (1998). A spectrin membrane skeleton of the Golgi complex. Biochim Biophys Acta 1404, 153–160.

Bernard O (2007). Lim kinases, regulators of actin dynamics. Int J Biochem Cell Biol 39, 1071–1076.

Bernstein BW, Bamburg JR (2010). ADF/cofilin: a functional node in cell biology. Trends Cell Biol 20, 187–195.

Bershadsky AD, Ballestrem C, Carramusa L, Zilberman Y, Gilquin B, Khochbin S, Alexandrova AY, Verkhovsky AB, Shemesh T, Kozlov MM (2006). Assembly and mechanosensory function of focal adhesions: experiments and models. Eur J Cell Biol 85, 165–173.

Brummelkamp TR, Bernards R, Agami R (2002). A system for stable expression of short interfering RNAs in mammalian cells. Science 296, 550–553.

Burkhardt JK (1998). The role of microtubule-based motor proteins in maintaining the structure and function of the Golgi complex. Biochim Biophys Acta 1404, 113–126.

Burkhardt JK, Echeverri CJ, Nilsson T, Vallee RB (1997). Overexpression of the dynamitin (p50) subunit of the dynactin complex disrupts dynein-dependent maintenance of membrane organelle distribution. J Cell Biol 139, 469–484.

Camera P, da Silva JS, Griffiths G, Giuffrida MG, Ferrara L, Schubert V, Imarisio S, Silengo L, Dotti CG, Di Cunto F (2003). Citron-N is a neuronal Rho-associated protein involved in Golgi organization through actin cytoskeleton regulation. Nat Cell Biol 5, 1071–1078.

Campellone KG, Webb NJ, Znameroski EA, Welch MD (2008). WHAMM is an Arp2/3 complex activator that binds microtubules and functions in ER to Golgi transport. Cell 134, 148–161.

Carramusa L, Ballestrem C, Zilberman Y, Bershadsky AD (2007). Mammalian diaphanous-related formin Dia1 controls the organization of E-cadherin-mediated cell-cell junctions. J Cell Sci 120, 3870–3882.

Chabin-Brion K, Marceiller J, Perez F, Settegrana C, Drechou A, Durand G, Pous C (2001). The Golgi complex is a microtubule-organizing organelle. Mol Biol Cell 12, 2047–2060.

Chesarone MA, DuPage AG, Goode BL (2010). Unleashing formins to remodel the actin and microtubule cytoskeletons. Nat Rev Mol Cell Biol 11, 62–74.

Chhabra ES, Higgs HN (2007). The many faces of actin: matching assembly factors with cellular structures. Nat Cell Biol 9, 1110–1121.

Cole NB, Sciaky N, Marotta A, Song J, Lippincott-Schwartz J (1996). Golgi dispersal during microtubule disruption: regeneration of Golgi stacks at peripheral endoplasmic reticulum exit sites. Mol Biol Cell 7, 631–650.

Corthesy-Theulaz I, Pauloin A, Pfeffer SR (1992). Cytoplasmic dynein participates in the centrosomal localization of the Golgi complex. J Cell Biol 118, 1333–1345.

De Matteis MA, Morrow JS (2000). Spectrin tethers and mesh in the biosynthetic pathway. J Cell Sci 113, Pt 132331–2343.

Del Nery E, Miserey-Lenkei S, Falguieres T, Nizak C, Johannes L, Perez F, Goud B (2006). Rab6A and Rab6A' GTPases play non-overlapping roles in membrane trafficking. Traffic 7, 394–407.

Dippold HC *et al*. (2009). GOLPH3 bridges phosphatidylinositol-4-phosphate and actomyosin to stretch and shape the Golgi to promote budding. Cell 139, 337–351.

Echard A, Jollivet F, Martinez O, Lacapere JJ, Rousselet A, Janoueix-Lerosey I, Goud B (1998). Interaction of a Golgi-associated kinesin-like protein with Rab6. Science 279, 580–585.

Efimov A *et al*. (2007). Asymmetric CLASP-dependent nucleation of noncentrosomal microtubules at the trans-Golgi network. Dev Cell 12, 917–930.

Fernandez-Borja M, Janssen L, Verwoerd D, Hordijk P, Neefjes J (2005). RhoB regulates endosome transport by promoting actin assembly on endosomal membranes through Dia1. J Cell Sci 118, 2661–2670.

Foletta VC, Moussi N, Sarmiere PD, Bamburg JR, Bernard O (2004). LIM kinase 1, a key regulator of actin dynamics, is widely expressed in embryonic and adult tissues. Exp Cell Res 294, 392–405.

Girod A, Storrie B, Simpson JC, Johannes L, Goud B, Roberts LM, Lord JM, Nilsson T, Pepperkok R (1999). Evidence for a COP-I-independent transport route from the Golgi complex to the endoplasmic reticulum. Nat Cell Biol 1, 423–430.

Glick BS, Nakano A (2009). Membrane traffic within the Golgi apparatus. Annu Rev Cell Dev Biol 25, 113–132.

Goode BL, Eck MJ (2007). Mechanism and function of formins in the control of actin assembly. Annu Rev Biochem 76, 593–627.

Grigoriev I *et al*. (2007). Rab6 regulates transport and targeting of exocytotic carriers. Dev Cell 13, 305–314.

Gupta V, Palmer KJ, Spence P, Hudson A, Stephens DJ (2008). Kinesin-1 (uKHC/KIF5B) is required for bidirectional motility of ER exit sites and efficient ER-to-Golgi transport. Traffic 9, 1850–1866.

Helfman DM, Levy ET, Berthier C, Shtutman M, Riveline D, Grosheva I, Lachish-Zalait A, Elbaum M, Bershadsky AD (1999). Caldesmon inhibits nonmuscle cell contractility and interferes with the formation of focal adhesions. Mol Biol Cell 10, 3097–3112.

Higashida C, Miyoshi T, Fujita A, Oceguera-Yanez F, Monypenny J, Andou Y, Narumiya S, Watanabe N (2004). Actin polymerization-driven molecular movement of mDia1 in living cells. Science 303, 2007–2010.

Holleran EA, Holzbaur EL (1998). Speculating about spectrin: new insights into the Golgi-associated cytoskeleton. Trends Cell Biol 8, 26–29.

Hoppeler-Lebel A, Celati C, Bellett G, Mogensen MM, Klein-Hitpass L, Bornens M, Tassin AM (2007). Centrosomal CAP350 protein stabilises microtubules associated with the Golgi complex. J Cell Sci 120, 3299–3308.

Hoshino H, Tamaki A, Yagura T (1997). Process of dispersion and fragmentation of Golgi complex by microtubule bundles formed in Taxol treated HeLa cells. Cell Struct Funct 22, 325–334.

Kang Q, Wang T, Zhang H, Mohandas N, An X (2009). A Golgi-associated protein 4.1B variant is required for assimilation of proteins in the membrane. J Cell Sci 122, 1091–1099.

Kozlov MM, McMahon HT, Chernomordik LV (2010). Protein-driven membrane stresses in fusion and fission. Trends Biochem Sci 35, 699–706.

Lazaro-Dieguez F, Jimenez N, Barth H, Koster AJ, Renau-Piqueras J, Llopis JL, Burger KN, Egea G (2006). Actin filaments are involved in the maintenance of Golgi cisternae morphology and intra-Golgi pH. Cell Motil Cytoskeleton 63, 778–791.

Levenberg S, Katz BZ, Yamada KM, Geiger B (1998). Long-range and selective autoregulation of cell-cell or cell-matrix adhesions by cadherin or integrin ligands. J Cell Sci 111, Pt 3347–357.

Li F, Higgs HN (2003). The mouse formin mDia1 is a potent actin nucleation factor regulated by autoinhibition. Curr Biol 13, 1335–1340.

Luini A, Mironov AA, Polishchuk EV, Polishchuk RS (2008). Morphogenesis of post-Golgi transport carriers. Histochem Cell Biol 129, 153–161.

Magdalena J, Millard TH, Machesky LM (2003). Microtubule involvement in NIH 3T3 Golgi and MTOC polarity establishment. J Cell Sci 116, 743–756.

Martinez O, Antony C, Pehau-Arnaudet G, Berger EG, Salamero J, Goud B (1997). GTP-bound forms of rab6 induce the redistribution of Golgi proteins into the endoplasmic reticulum. Proc Natl Acad Sci USA 94, 1828–1833.

Miller PM, Folkmann AW, Maia AR, Efimova N, Efimov A, Kaverina I (2009). Golgi-derived CLASP-dependent microtubules control Golgi organization and polarized trafficking in motile cells. Nat Cell Biol 11, 1069–1080.

Minin AA, Kulik AV, Gyoeva FK, Li Y, Goshima G, Gelfand VI (2006). Regulation of mitochondria distribution by RhoA and formins. J Cell Sci 119, 659–670.

Miserey-Lenkei S, Chalancon G, Bardin S, Formstecher E, Goud B, Echard A (2010). Rab and actomyosin-dependent fission of transport vesicles at the Golgi complex. Nat Cell Biol 12, 645–654.

Morton WM, Ayscough KR, McLaughlin PJ (2000). Latrunculin alters the actin-monomer subunit interface to prevent polymerization. Nat Cell Biol 2, 376–378.

Narumiya S, Tanji M, Ishizaki T (2009). Rho signaling, ROCK and mDia1, in transformation, metastasis and invasion. Cancer Metastasis Rev 28, 65–76.
Paran Y, Lavelin I, Naffar-Abu-Amara S, Winograd-Katz S, Liron Y, Geiger B, Kam Z (2006). Development and application of automatic high-resolution light microscopy for cell-based screens. Methods Enzymol 414, 228–247.
Percival JM, Hughes JA, Brown DL, Schevzov G, Heimann K, Vrhovski B, Bryce N, Stow JL, Gunning PW (2004). Targeting of a tropomyosin isoform to short microfilaments associated with the Golgi complex. Mol Biol Cell 15, 268–280.
Ramirez IB, Lowe M (2009). Golgins and GRASPs: holding the Golgi together. Semin Cell Dev Biol 20, 770–779.
Ren XD, Kiosses WB, Schwartz MA (1999). Regulation of the small GTP-binding protein Rho by cell adhesion and the cytoskeleton. EMBO J 18, 578–585.
Riedl J *et al.* (2008). Lifeact: a versatile marker to visualize F-actin. Nat Methods 5, 605–607.
Rivero S, Cardenas J, Bornens M, Rios RM (2009). Microtubule nucleation at the cis-side of the Golgi apparatus requires AKAP450 and GM130. EMBO J 28, 1016–1028.
Rosso S, Bollati F, Bisbal M, Peretti D, Sumi T, Nakamura T, Quiroga S, Ferreira A, Caceres A (2004). LIMK1 regulates Golgi dynamics, traffic of Golgi-derived vesicles, and process extension in primary cultured neurons. Mol Biol Cell 15, 3433–3449.
Rothman JE (1981). The Golgi apparatus: two organelles in tandem. Science 213, 1212–1219.
Sahlender DA, Roberts RC, Arden SD, Spudich G, Taylor MJ, Luzio JP, Kendrick-Jones J, Buss F (2005). Optineurin links myosin VI to the Golgi complex and is involved in Golgi organization and exocytosis. J Cell Biol 169, 285–295.
Salvarezza SB, Deborde S, Schreiner R, Campagne F, Kessels MM, Qualmann B, Caceres A, Kreitzer G, Rodriguez-Boulan E (2009). LIM kinase 1 and cofilin regulate actin filament population required for dynamin-dependent apical carrier fission from the trans-Golgi network. Mol Biol Cell 20, 438–451.
Schiff PB, Horwitz SB (1980). Taxol stabilizes microtubules in mouse fibroblast cells. Proc Natl Acad Sci USA 77, 1561–1565.
Schroer TA (2004). Dynactin. Annu Rev Cell Dev Biol 20, 759–779.
Sengupta D, Truschel S, Bachert C, Linstedt AD (2009). Organelle tethering by a homotypic PDZ interaction underlies formation of the Golgi membrane network. J Cell Biol 186, 41–55.
Shi Y, Zhang J, Mullin M, Dong B, Alberts AS, Siminovitch KA (2009). The mDial formin is required for neutrophil polarization, migration, and activation of the LARG/RhoA/ROCK signaling axis during chemotaxis. J Immunol 182, 3837–3845.
Stauber T, Simpson JC, Pepperkok R, Vernos I (2006). A role for kinesin-2 in COPI-dependent recycling between the ER and the Golgi complex. Curr Biol 16, 2245–2251.
Storrie B, White J, Rottger S, Stelzer EH, Suganuma T, Nilsson T (1998). Recycling of Golgi-resident glycosyltransferases through the ER reveals a novel pathway and provides an explanation for nocodazole-induced Golgi scattering. J Cell Biol 143, 1505–1521.
Sutterlin C, Colanzi A (2010). The Golgi and the centrosome: building a functional partnership. J Cell Biol 188, 621–628.
Thyberg J, Moskalewski S (1985). Microtubules and the organization of the Golgi complex. Exp Cell Res 159, 1–16.
Thyberg J, Moskalewski S (1999). Role of microtubules in the organization of the Golgi complex. Exp Cell Res 246, 263–279.
Valderrama F, Babia T, Ayala I, Kok JW, Renau-Piqueras J, Egea G (1998). Actin microfilaments are essential for the cytological positioning and morphology of the Golgi complex. Eur J Cell Biol 76, 9–17.
Valderrama F, Luna A, Babia T, Martinez-Menarguez JA, Ballesta J, Barth H, Chaponnier C, Renau-Piqueras J, Egea G (2000). The Golgi-associated COPI-coated buds and vesicles contain beta/gamma-actin. Proc Natl Acad Sci U S A 97, 1560–1565.
Vicente-Manzanares M, Ma X, Adelstein RS, Horwitz AR (2009). Non-muscle myosin II takes centre stage in cell adhesion and migration. Nat Rev Mol Cell Biol 10, 778–790.
von Blume J, Duran JM, Forlanelli E, Alleaume AM, Egorov M, Polishchuk R, Molina H, Malhotra V (2009). Actin remodeling by ADF/cofilin is required for cargo sorting at the trans-Golgi network. J Cell Biol 187, 1055–1069.
Wallar BJ, Deward AD, Resau JH, Alberts AS (2007). RhoB and the mammalian Diaphanous-related formin mDia2 in endosome trafficking. Exp Cell Res 313, 560–571.
Warner CL, Stewart A, Luzio JP, Steel KP, Libby RT, Kendrick-Jones J, Buss F (2003). Loss of myosin VI reduces secretion and the size of the Golgi in fibroblasts from Snell's waltzer mice. EMBO J 22, 569–579.
Watanabe N, Kato T, Fujita A, Ishizaki T, Narumiya S (1999). Cooperation between mDia1 and ROCK in Rho-induced actin reorganization. Nat Cell Biol 1, 136–143.
Watanabe N, Madaule P, Reid T, Ishizaki T, Watanabe G, Kakizuka A, Saito Y, Nakao K, Jockusch BM, Narumiya S (1997). p140mDia, a mammalian homolog of *Drosophila* diaphanous, is a target protein for Rho small GTPase and is a ligand for profilin. EMBO J 16, 3044–3056.
Wehland J, Henkart M, Klausner R, Sandoval IV (1983). Role of microtubules in the distribution of the Golgi apparatus: effect of taxol and microinjected anti-alpha-tubulin antibodies. Proc Natl Acad Sci USA 80, 4286–4290.
White J *et al.* (1999). Rab6 coordinates a novel Golgi to ER retrograde transport pathway in live cells. J Cell Biol 147, 743–760.
Xu Y, Takeda S, Nakata T, Noda Y, Tanaka Y, Hirokawa N (2002). Role of KIFC3 motor protein in Golgi positioning and integration. J Cell Biol 158, 293–303.
Yamana N *et al.* (2006). The Rho-mDia1 pathway regulates cell polarity and focal adhesion turnover in migrating cells through mobilizing Apc and c-Src. Mol Cell Biol 26, 6844–6858.
Zilberman Y, Ballestrem C, Carramusa L, Mazitschek R, Khochbin S, Bershadsky A (2009). Regulation of microtubule dynamics by inhibition of the tubulin deacetylase HDAC6. J Cell Sci 122, 3531–3541.